Journal of Photochemistry and Photobiology A: Chemistry 224 (2011) 25–30

Contents lists available at SciVerse ScienceDirect

Journal of Photochemistry and Photobiology A: Chemistry

journal homepage: www.elsevier.com/locate/jphotochem

Expanding the photoresponse range of TiO_2 nanotube arrays by CdS/CdSe/ZnS quantum dots co-modification

Zi-Xia Li, Yu-Long Xie, Hua Xu, Tian-Ming Wang, Zhu-Guo Xu*, Hao-Li Zhang*

State Key Laboratory of Applied Organic Chemistry, College of Chemistry and Chemical Engineering, Lanzhou University, Lanzhou 730000, China

ARTICLE INFO

Article history:
Received 26 March 2011
Received in revised form 24 July 2011
Accepted 5 September 2011
Available online 13 September 2011

Keywords:
TiO_2 nanotube
CdS
CdSe
ZnS
Sensitization
Solar cell

ABSTRACT

Highly ordered TiO_2 nanotube arrays modified by CdS, CdSe and ZnS quantum dots (QDs) were fabricated by using chemical bath deposition. The CdS and CdSe QDs modification expands the photoresponse range of TiO_2 nanotube arrays from ultraviolet region to visible range. It is demonstrated that sequentially assembled CdS and CdSe QDs significantly improved the light harvesting ability and photocurrent efficiency, and a high incident photon to current conversion efficiency (IPCE) of 53% was obtained. Further coating the TiO_2/CdS/CdSe nanotube array with a barrier layer of ZnS QD increases the IPCE to 72%. The improved photo harvest efficiency of the CdS/CdSe/ZnS co-modified TiO_2 arrays is attributed to the formation of an ideal cascade-type energy band structure, which is advantageous for both electron injection and hole recovery.

1. Introduction

Dye-sensitized solar cells (DSSCs) has attracted great interest as a potential low cost and high efficiency alternative to the Si based solar cell [1]. Most DSSCs have been constructed based on organic or organometallic dye-sensitized colloidal TiO_2 films. In addition to the organic sensitizers, semiconductor quantum dots (QDs) can also serve as sensitizers to construct quantum dot sensitized solar cells (QDSSCs). Semiconductor QDs, such as CdS [2,3], CdSe [4,5], CdTe [6], PbS [7] and PbSe [8], have many potential advantages, including high stability, absorb light in the visible region, tunable band gaps [9], high molar extinction coefficients [10], and large intrinsic dipole moments enhancing charge separation [11]. Therefore, QDSSCs have attracted great attention in the past decade. Most of the researches on QDSSCs have been carried out using colloidal TiO_2 films as the photoanode, and the focus has been the design of the QD/TiO_2 interface for achieving high quantum efficiency. For example, Grätzel group had assembled CdSe QDs onto mesoscopic TiO_2 films via a molecular linker, and achieved an unprecedented IPCE of 36% and an overall conversion efficiency of over 1.7% [12]. Li et al. reported that the combination of CdSe QD sensitization and N-doping of TiO_2 nanoparticles could increase the photovoltaic response due to the synergistic effect [13]. Despite the potential advantages of QDSSCs, they have not achieved better efficiencies compared to conventional DSSCs. Therefore, more investigations are needed to explore the full potential of QDSSCs.

One potential method for improving the performance of QDSSCs is by constructing desired energy band structures using multiple QDs. Hodes and co-workers have firstly demonstrated that a desired cascade structure can be formed by sequential deposition of CdS and CdSe layers onto the TiO_2 nanoparticle films [14]. Recently, Lee et al. have also reported a self-assembled TiO_2/CdS/CdSe structure that exhibited a significant enhancement in the photocurrent response [15,16]. Another promising method that has been proposed recently is based on replacing the conventional TiO_2 nanoparticle films with highly order TiO_2 nanotube (NT) arrays. The structural disorders and vast grain boundaries of TiO_2 nanoparticle film bring some obstacles to the electron transport and affect the charge separation efficiency. Comparing to TiO_2 nanoparticles, TiO_2 NT arrays with aligned porosity, high crystallinity, and oriented nature are advantaged in the efficiency of charge collection by promoting both more rapid electron transport and slower charge recombination. Chen et al. have suggested that DSSC based on TiO_2 NT arrays outperform conventional nanoparticle-based DSSC, and the photovoltaic performance of the NT-based DSSC devices enhanced as increasing the tube length [17]. Kamat et al. confirmed the improvement in the photoconversion efficiency by facilitating the charge transport through TiO_2 NT architecture constructing an interesting rainbow solar cell to further improve the light

* Corresponding authors. Tel.: +86 931 8912365; fax: +86 931 8912365.
E-mail addresses: Xuzhg@lzu.edu.cn (Z.-G. Xu), Haoli.Zhang@lzu.edu.cn (H.-L. Zhang).

1010-6030/$ – see front matter © 2011 Elsevier B.V. All rights reserved.
doi:10.1016/j.jphotochem.2011.09.002

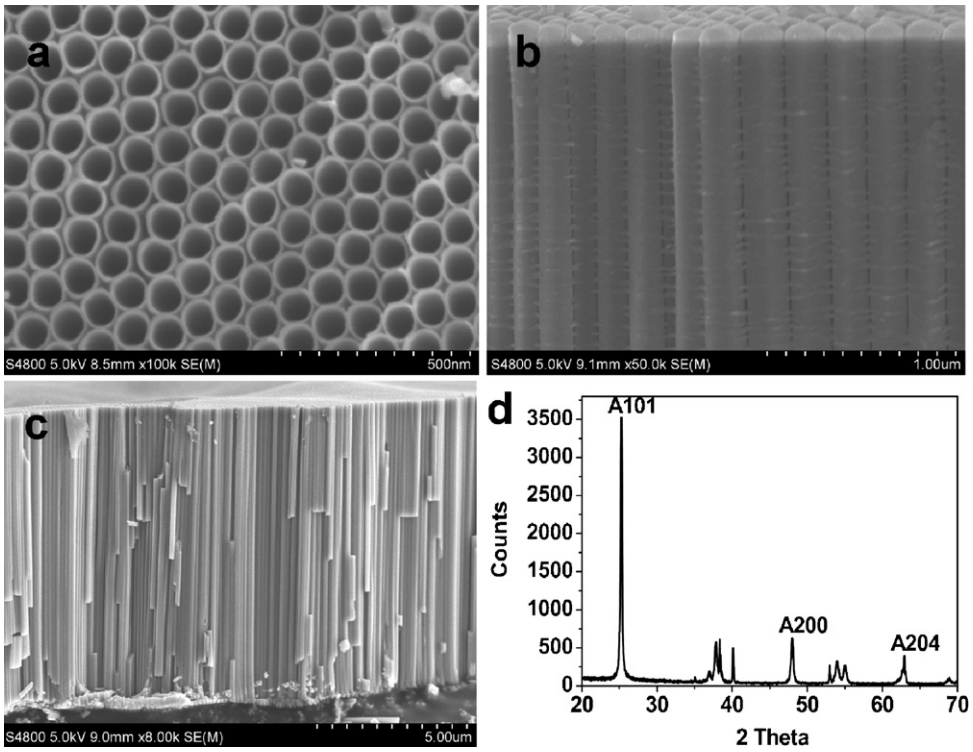

Fig. 1. FESEM images of TiO_2 NTs. (a) The top view of perfectly aligned TiO_2 NTs, (b, c) cross-sectional view of the TiO_2 NTs, (d) XRD patterns of TiO_2 NTs after being annealed at 450 °C for 3 h. Reference peaks for anatase are annotated with A.

harvesting capability [18]. In our previous work, we have shown that CdSe QD assembled onto TiO_2 NTs can significantly enhance its photoresponse [19].

However, there has been few investigation on constructing cascade-type QD assembly on TiO_2 NTs [20]. In this work, we studied the effects of co-modification by CdS, CdSe and ZnS QDs on the photovoltaic response of TiO_2 NT-based QDSSC. Highly ordered TiO_2 NT arrays were fabricated by electrochemical anodization [21]. The TiO_2 NT arrays were treated by sequential chemical bath deposition (CBD) of CdS, CdSe and ZnS QDs and were used as photoanodes in QDSSC. We demonstrated that the co-modified TiO_2 NT arrays possess superior photovoltaic response compared to the single QD sensitized devices, and the final TiO_2/CdS/CdSe/ZnS photoanode leads to high efficiency QDSSCs.

2. Experimental

2.1. Fabrication of TiO_2 NT arrays

The 0.25 mm thick titanium foils (99.95%, Alfa Aesar) were degreased by successively sonicating for 10 min in acetone, isopropanol, and finally methanol, then dried under a flowing N_2 stream. For the anodic growth experiments, highly ordered TiO_2 NT arrays were prepared by a potentiostatic anodization in a two-electrode electrochemical cell. A titanium foil with a size of $1 \times 3\,cm^2$ was used as a working electrode and a platinum foil served as a counter electrode. These foils were anodized at a direct voltage in an electrolyte containing ethylene glycol, 2 vol%, and 0.3 wt% NH_4F. The samples were anodized at 60 V for 2 h, then rinsed with distilled water and dried in the air. The as-prepared TiO_2 NT films were annealed under an air atmosphere at 450 °C for 3 h. The annealed TiO_2 NT film was immersed in the $TiCl_4$ solution for half an hour at 50 °C, then annealed at 400 °C for 1 h in the air.

2.2. Deposition of CdS, CdSe and ZnS QDs

The highly ordered TiO_2 NTs were sequentially sensitized with CdS and CdSe QDs by using CBD (chemical bath deposition) method. First, a TiO_2 NT film was dipped into 0.5 M $Cd(CH_3COO)_2$ ethanol solution for 5 min, rinsed with ethanol, then dipped for another 5 min into a 0.5 M Na_2S methanol solution and again rinsed with methanol. The two-step dipping procedure is termed as one CBD cycle and the incorporated amount of CdS QDs can be increased by repeating the assembly cycles (a total of three cycles).

In the following CBD process of CdSe QDs, sodium selenosulphate (Na_2SeSO_3) was used as the Se source. The Na_2SeSO_3 aqueous solution was prepared by refluxing Se (0.3 M) in an aqueous solution of Na_2SO_3 (0.6 M) at 70 °C for 7 h. In the CBD process of CdSe QDs, the TiO_2/CdS (or bared TiO_2) samples were first dipped into 0.5 M $Cd(CH_3COO)_2$ ethanol solution for 5 min at room temperature, rinsed with ethanol, and then dipped into Na_2SeSO_3 solution for 5 min at 50 °C and rinsed again with pure water. The two-step dipping procedure is termed as one CBD cycle. Repeating the CBD cycle would increase the amount of CdSe QDs (a total of four cycles).

The CBD method was also used to deposit the ZnS passivation layer. The TiO_2/CdS/CdSe samples were coated with ZnS by twice dipping alternately into 0.1 M $Zn(NO_3)_2$ and 0.1 M Na_2S solutions for 1 min/dip, rinsing with pure water between dips (a total of two cycles). The chemical reactions for the formation of CdS, CdSe and ZnS QDs are given below:

$$Cd^{2+} + S^{2-} \rightarrow CdS \quad (1)$$

$$Cd^{2+} + SeSO_3{}^{2-} + 2OH^- \rightarrow CdSe + SO_4{}^{2-} + H_2O \quad (2)$$

$$Zn^{2+} + S^{2-} \rightarrow ZnS \quad (3)$$

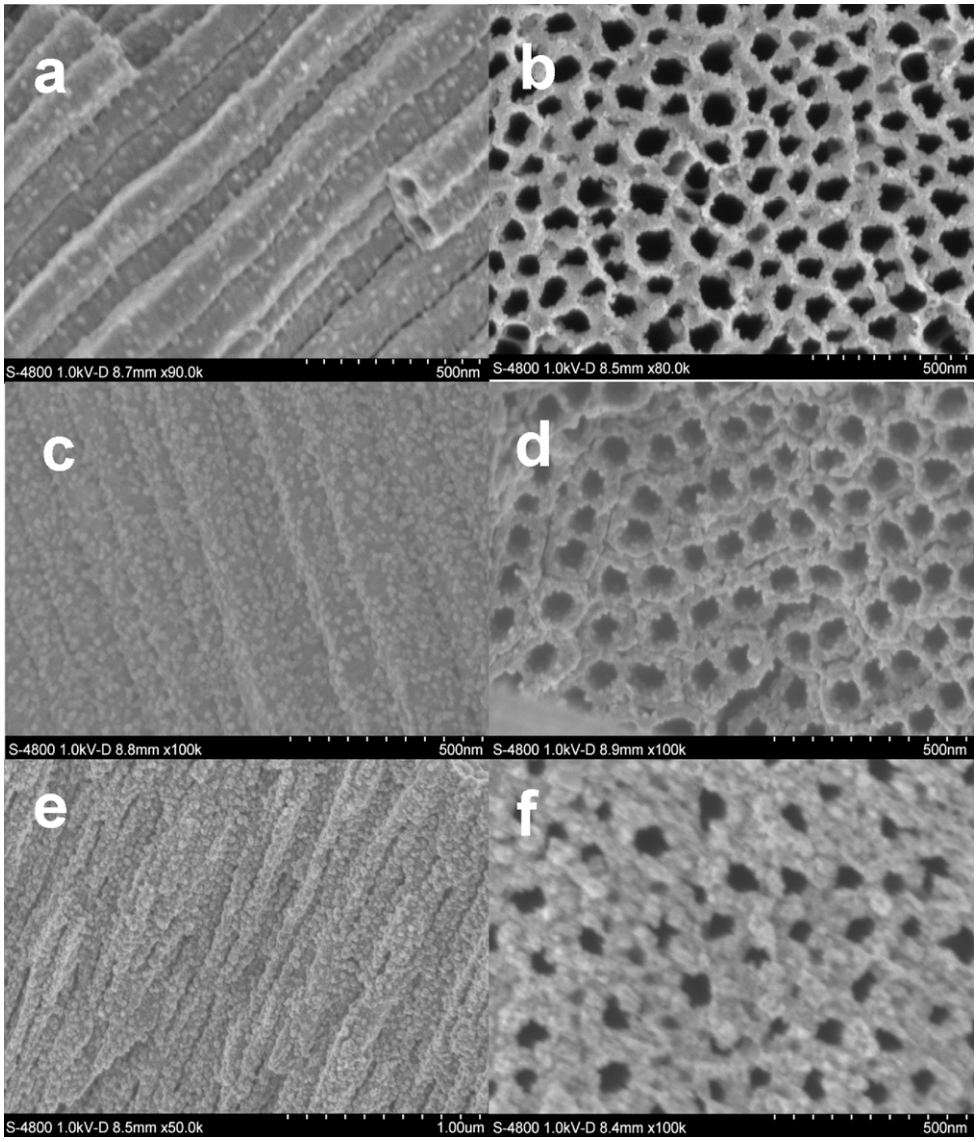

Fig. 2. FESEM images of various QD modified TiO_2 NT nanostructures. (a) The side view of the TiO_2/CdS, (b) the top view of TiO_2/CdS, (c) the side view of the TiO_2/CdS/CdSe, (d) the top view of the TiO_2/CdS/CdSe, (e) the side view of the TiO_2/CdS/CdSe/ZnS, (f) the top view of the TiO_2/CdS/CdSe/ZnS NT arrays.

2.3. Solar cell configuration

A QDSSC was assembled by sandwiching a sensitized TiO_2 NTs film photoelectrode and an Au-coated counter electrode using 60 μm thick sealing material (Surlyn). A polysulfide Na_2S_X redox electrolyte prepared using water/methanol (7:3 by volume) was used in this work. The electrolyte contains 0.5 M Na_2S, 0.1 M S and 0.2 M KCl. The active area of the cell is 0.5 cm^2.

2.4. Optical and electrical characterizations

The structural characterizations of the samples were carried out using field emission scanning electron microscopy (FESEM, Hitachi S-4800 microscope). The crystal structure of the TiO_2 NTs was examined by X-ray diffraction (XRD). The absorption spectra were recorded by a PE950 UV–vis spectrophotometer. The QDSSCs were illuminated by an AM 1.5 illumination provided by a xenon lamp (OSRAM E-O 150 W) with an optical filter (AM 1.5G) under 100 mW/cm^2 irradiation (calibrated by a standard silicon solar cell). The incident photon to current efficiency (IPCE) was measured by solar cell scan 100 (Zolix Instruments). The electrochemical set-up consisted of a three-electrode system in a quartz cell, using a saturated calomel electrode (SCE) as reference electrode, aqueous 0.1 M Na_2S solution as a redox couple. The photocurrent–voltage (I–V) measurement was conducted using an electrochemistry work station (CHI660b).

3. Results and discussion

Shown in Fig. 1(a–c) are the FESEM images of TiO_2 NTs. The top view image (Fig. 1a) shows highly uniform porous morphology with the average inner diameter of nanotubes around 120 nm. In Fig. 1(b and c), with nanotubular structure underneath, the TiO_2 NTs have a vertically oriented structure without bundling. Fig. 1(c) is a cross-sectional image showing that the NTs are well aligned with an average length of about 12 μm. The crystal structure of the TiO_2 NT sample was examined by XRD experiments. As shown in Fig. 1(d), all diffraction peaks can be well-indexed by the anatase phase of TiO_2 and Ti metal phase.

For photovoltaic applications, the structure of the QD adsorbed NTs should meet at less two criteria. First, the QDs should be uniformly deposited onto the NT surface without aggregation, so that

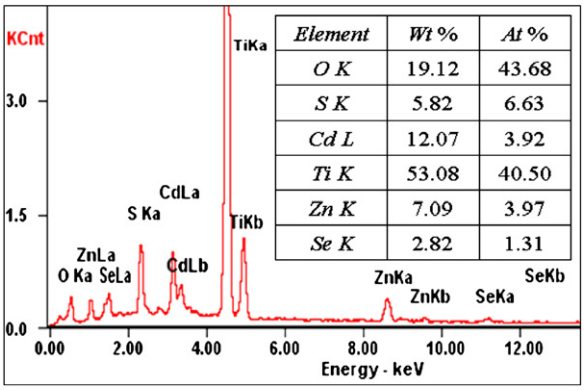

Element	Wt %	At %
O K	19.12	43.68
S K	5.82	6.63
Cd L	12.07	3.92
Ti K	53.08	40.50
Zn K	7.09	3.97
Se K	2.82	1.31

Fig. 3. UV–vis absorption spectra of bare TiO_2 NTs film and TiO_2 NTs films modified by various QDs.

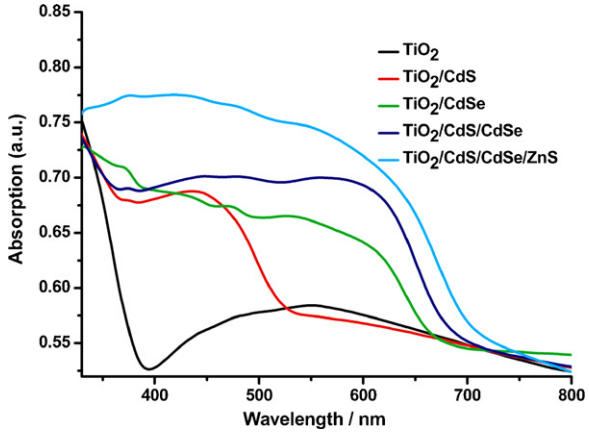

Fig. 4. IPCE curves of various QDs modified electrodes.

the area of QD/TiO_2 contact can be maximized. Second, a moderate amount the QDs should be deposited so that the tubes are not blocked. Fig. 2 shows the surface morphology of TiO_2 NT arrays modified by various QDs via the CBD process. The side view of the CdS-deposited TiO_2 NTs in Fig. 2(a) reveals that many CdS QDs are adsorbed onto the side walls of TiO_2 NTs. The CdS QDs are well-distributed on the tube sidewall without aggregation. The CdS QDs are nearly mono-disperse in size distribution and the mean diameters of CdS QDs were measured to be around 20 nm. Fig. 2(b) shows that CdS QDs are deposited mainly along the side walls of the TiO_2 NTs. The amount of the deposited CdS QDs was controlled by the reaction time, and the pores remain well open. The structure of the CdSe/TiO_2 is similar to that of the CdS/TiO_2. Fig. 2(c) shows the FESEM images of the CdS/CdSe co-sensitized TiO_2 NTs. It can be seen that a large amount of CdSe are deposited onto the sidewalls of TiO_2 NTs after the first CdS layer. The diameter of CdSe QDs is estimated to be 20 nm. Besides, it was found from the experiment that the deposition of the CdSe layer onto the TiO_2/CdS is much faster than that on the as prepared TiO_2 NTs, which suggests that the CdSe QDs are much more favorable to be deposited onto CdS QDs. The top view of the TiO_2/CdS/CdSe in Fig. 2(d) proves that the nanoparticles were deposited inside the nanotubes, while the pore was not blocked. At last, a layer of ZnS QDs was assembled to give the TiO_2/CdS/CdSe/ZnS structure. More nanoparticles can be observed in Fig. 2(e), and the size of the ZnS QDs is slightly larger than that of the CdS and CdSe QDs. Fig. 2(f) shows that the top of the NTs remains open after all the deposition steps completed, which are important for the electrolyte transport.

The sample compositions were studied by energy dispersive X-ray spectroscopy (EDS) analysis (Fig. 3). The Ti and O peaks are from the TiO_2 NTs; and the Cd, Se, and S peaks, clearly visible in the EDS spectrum, are from the QDs. Quantitative analysis of the EDS spectrum (the inset of Fig. 3) reveals that the atomic ratio of Cd plus Zn versus S plus Se is nearly 1, indicating that the deposited CdS and CdSe QDs are likely to be stoichiometric.

The optical properties of the five electrodes are studied by their UV–vis absorption spectra. The absorption edge, obtained from the intersection of the sharply decreasing region of a spectrum with its baseline, of the as prepared TiO_2 NT films extended to around 380 nm (Fig. 4), corresponding to a band gap of 3.2 eV of anatase TiO_2. The absorption edges locate at 518 nm for the TiO_2/CdS, and 683 nm for the TiO_2/CdSe electrodes, corresponding to band gaps of 2.39 and 1.80 eV, respectively [22]. These band gaps are wider than the values reported for bulk CdS and CdSe (2.25 and 1.7 eV, respectively), which could be attributed to the quantum confinement effect of the QDs. The absorbance of the co-sensitized TiO_2/CdS/CdSe film is higher than that of either the TiO_2/CdS or the TiO_2/CdSe film, which result is reproducible under carefully controlled experimental conditions. The enhanced absorption is likely indicating that the TiO_2/CdS/CdSe have complementary and enhancement effects due to the wider absorption of CdSe and the good charge transport mobility of CdS [16]. After coating a layer of ZnS shell, the absorption is sharply increased and a red shift of the absorption edge is observed, which is similar to the previous observation on the CdSe/ZnS core-shell structure [23].

To study the photocurrent performance of these QD modified TiO_2 NT electrodes under different wavelengths, experiments were conducted to obtain the IPCE. IPCE is also referred to as external quantum efficiency (EQE), which is the ratio of electrons collected per incident photon (with no correction for reflection losses). IPCE can be used as a measure of the efficiency of charge transport [24]. The equation for calculating IPCE is given by [5]:

$$\text{IPCE}\ (\%) = \left(\frac{1240 \times J_{sc}}{\lambda P_{in}}\right) \times 100 \qquad (4)$$

where J_{sc} is the photocurrent density, P_{in} is the intensity of the light, and λ is the wavelength of the incident light.

Fig. 5 illustrates that the sensitization by both the CdS and CdSe QDs significantly expands the photoresponse region of the TiO_2 NT electrode. The photoresponse wavelengths of the TiO_2/CdS and TiO_2/CdSe electrodes extend to about 550 nm and 700 nm, respectively, which correspond well with their above absorption spectra. The maximum IPCEs are 20% for the TiO_2/CdS at 416 nm, and 39% for the TiO_2/CdSe electrode at 607 nm. Co-sensitization by both the CdS and CdSe QDs gives much higher photoresponse compared to the single QD sensitized TiO_2 NTs, and the TiO_2/CdS/CdSe electrode exhibits a maximum IPCE of 53% around 491 nm. The IPCE spectrum of the TiO_2/CdS/CdSe electrode is consistent with

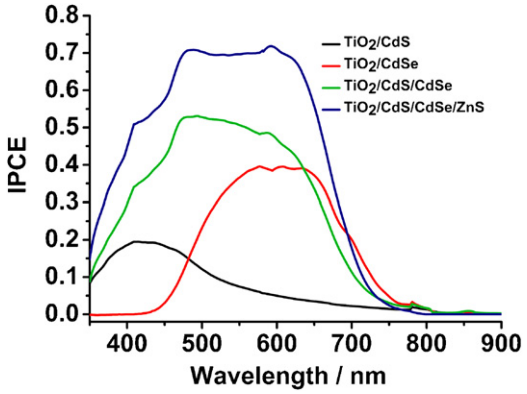

Fig. 5. Linear sweep voltammagrams of photoanodes fabricated from various QDs modified electrodes at a scan rate of 50 mV/s.

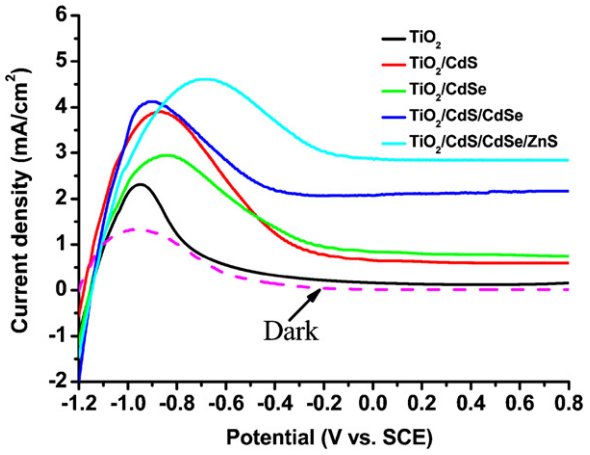

Fig. 6. (a) Relative energy levels of TiO_2, CdS, CdSe, and ZnS in bulk phase, (b) the proposed energy band structure of the TiO_2/CdS/CdSe/ZnS nanostructure interface. All the energy levels are referenced to NHE scale. CB and VB are conduction band and valence band.

its UV–vis absorption spectrum. Though the light harvest region of TiO_2/CdS/CdSe is similar to that of TiO_2/CdSe, but a dramatic increase in IPCE is obtained compared to both the TiO_2/CdS and TiO_2/CdSe electrodes. The high performance of the TiO_2/CdS/CdSe electrode is mainly attributed to a synergistic effect of the high electron injection efficiency of the CdS QDs and the wide light harvesting range of the CdSe QDs. The highest photocurrent response was obtained on the TiO_2/CdS/CdSe/ZnS photoelectrode, which gave a maximum IPCE of 72% at around 590 nm. This maximum IPCE value is higher than that of most QD modified TiO_2 photoanodes reported previously [4,5,12,16,18,25]. The only higher IPCE value was reported by Niitsoo et al. on a CdS and CdSe modified TiO_2 colloid electrode, which reached 80% [14].

Fig. 6 shows a set of linear sweep voltammagrams recorded from these photoanodes. Pristine TiO_2 NTs show relatively low steady photocurrent, ~0.144 mA/cm^2 at 0 V, due to the limited absorption of visible light. The shape of these voltammagrams of QD modified TiO_2 nanotubes is similar to those obtained previously on CdSe modified TiO_2 nanostructures [13]. Both the CdS QD and CdSe QD sensitized TiO_2 NTs samples exhibit substantially enhanced photocurrent compared to the pristine TiO_2 NTs, ~0.652 mA/cm^2 and ~0.841 mA/cm^2 at 0 V, respectively. This can be attributed to the improved visible light absorption by the QDs, as shown in the UV–vis absorption spectra. Significantly, the co-sensitized TiO_2/CdS/CdSe photoanode shows a much higher photocurrent density of ~2.074 mA/cm^2 at 0 V, which is three times larger than that of the TiO_2/CdS, and beyond two times larger than that of the TiO_2/CdSe. The voltammagram data indicates efficient interfacial charge transfer between the CdS, CdSe QDs and the TiO_2 NTs [20]. More importantly, the synergistic effect of the co-sensitized sample leads to a strong photocurrent enhancement. TiO_2/CdS/CdSe/ZnS photoanode exhibits the largest photocurrent density of ~2.869 mA/cm^2 at 0 V. This result corresponds well to the IPCE in Fig. 5, that the coating of the ZnS QDs clearly improves the photocurrent.

To understand the above observed results, a relative energy level of different components is shown in Fig. 7(a). According to the data reported in the literatures [26,27], the band gap of TiO_2 (3.2 eV) limits its absorption range below the wavelength of about 400 nm. CdS has a higher conduction band edge than TiO_2, which is favorable for electron injection. However, with a band gap of 2.25 eV, the absorption of bulk CdS is also limited below approximately 550 nm. Bulk CdSe has a band gap of 1.7 eV, which can extend the absorption to the whole visible region. The conduction band of CdSe is slightly lower than that of CdS. Lee and Lo have reported that when CdS and CdSe were brought in contact as a cascade structure, the electrons would flow from CdS to CdSe [15]. The re-distribution of the electrons leads a stepwise band structure. The insertion of a CdS layer between TiO_2 and CdSe elevates the conduction band of CdSe, leading a higher driving force for the electron transportation. In addition, quantum confinement effect makes the energy level of the conduction band more negative with the decreasing particle size [18]. As a result, an ideal model for the co-sensitized TiO_2 electrode is shown in Fig. 7(b). After the CdS and CdSe QDs are sequentially deposited onto a TiO_2 NT film, a cascade-type energy band structure is constructed for the co-sensitized photoanode. The best electron transport path is from the conduction band of CdSe to that of CdS, and finally reaching the conduction band of TiO_2. Meanwhile, this stepwise structure is also favorable for the hole transport. As a result, a higher IPCE and photocurrent density are obtained on the TiO_2/CdS/CdSe electrode.

Besides, a higher and broader absorption is also obtained on the TiO_2/CdS/CdSe electrode. After coating a layer ZnS QDs, the photoresponse is significantly improved, which could be attributed to several reasons. First, as the absorption edge of ZnS is at about 345 nm, a higher absorption can be obtained due to the complement of the absorption spectrum of the ZnS with that of the CdSe and CdS QDs. Second, ZnS acts as a passivation layer to protect the CdS and CdSe QDs from photocorrosion. Thus, the photoexcited electrons can efficiently transfer into the conduction band of TiO_2. Third, the outer ZnS layer can also be considered to be a potential barrier between the interface of QDs materials and the electrolyte. ZnS has a very wide band gap of 3.6 eV, it is much wider than that of the CdS and CdSe QDs. As a result, the leakage of electrons from

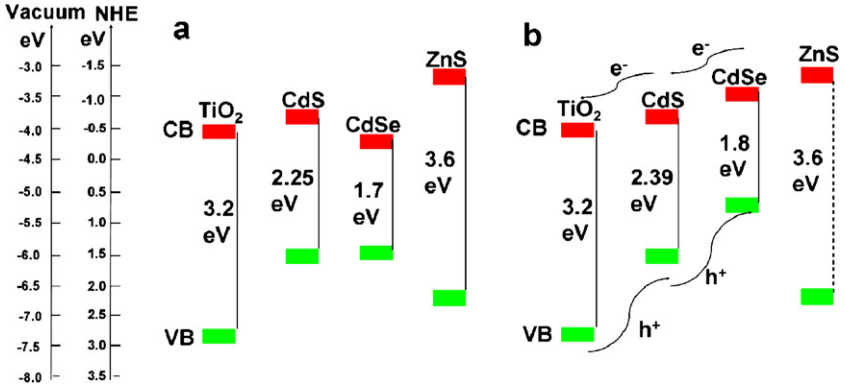

Fig. 7. (a) Relative energy levels of TiO_2, CdS, CdSe, and ZnS in bulk phase, (b) the proposed energy band structure of the TiO_2/CdS/CdSe/ZnS nanostructure interface. All the energy levels are referenced to NHE scale. CB and VB are conduction band and valence band.

the CdS and CdSe QDs into the electrolyte can be inhibited. Consequently, a much higher IPCE and photocurrent density can be obtained.

4. Conclusion

We have successfully fabricated a new type of TiO_2 NTs array photoanode, which is sequentially modified by CdS, CdSe and ZnS QDs. The co-sensitized electrode exhibited significantly improved photoresponse compared to the single type QD sensitized electrodes, including both expanded spectral response range and enhanced IPCE performance. Such improvement is mainly attributed to the overlap of the absorption spectra of the different materials and the formation of an ideal stepwise band structure which is advantageous to the transport of excited electrons and holes across the composite electrode. The resulted TiO_2/CdS/CdSe/ZnS photoanode exhibits a photoresponse range up to 730 nm and a maximum IPCE value of 72%. It is believed that such highly ordered array of TiO_2/CdS/CdSe/ZnS NTs could find application in high efficiency photovoltaic and photocatalysis applications.

Acknowledgement

This work is supported by National Natural Science Foundation of China (NSFC: 20872055, 21073079, J0730425), Chunhui project and 111 project.

References

[1] B.O. Regan, M. Grätzel, A low-coast, high-efficiency solar cell based on dye-sensitized colloidal TiO_2 films, Nature 353 (1991) 737–740.
[2] P. Sudhagar, J.H. Jung, S. Park, R. Sathyamoorthy, H. Ahn, Y.S. Kang, Self-assembled CdS quantum dots-sensitized TiO_2 nanospheroidal solar cells: structural and charge transport analysis, Electrochim. Acta 55 (2009) 113–117.
[3] Y.J. Chi, H.G. Fu, L. Hui, K.Y. Shi, H.B. Zhang, H.T. Yu, Preparation and photoelectric performance of ITO/TiO_2/CdS composite thin films, J. Photochem. Photobiol. A 195 (2008) 357–363.
[4] I. Robel, V. Subramanian, M. Kuno, P.V. Kamat, Quantum dot solar cells. Harvesting light energy with CdSe nanocrystals molecularly linked to mesoscopic TiO_2 films, J. Am. Chem. Soc. 128 (2006) 2385–2393.
[5] M.F. Hossain, S. Biswas, Z.H. Zhang, T. Takahashi, Bubble-like CdSe nanoclusters sensitized TiO_2 nanotube arrays for improvement in solar cell, J. Photochem. Photobiol. A 217 (2011) 68–75.
[6] J.H. Bang, P.V. Kamat, QDSC, A tale of two semiconductor nanocrystals: CdSe and CdTe, ACS Nano. 3 (2009) 1467–1476.
[7] H. Lee, H.C. Leventis, S.J. Moon, P. Chen, S. Ito, S.A. Haque, T. Torres, F. Nüesch, T. Geiger, S.M. Zakeeruddin, M. Grätzel, M.K. Nazeeruddin, PbS and CdS quantum dot-sensitized solid-state solar cells: old concepts, new results, Adv. Funct. Mater. 19 (2009) 2735–2742.
[8] M. Law, M.C. Beard, S. Choi, J.M. Luther, M.C. Hanna, A.J. Nozik, Determining the internal quantum efficiency of PbSe nanocrystal solar cells with the aid of an optical model, Nano Lett. 8 (2008) 3904–3910.
[9] I. Robel, M. Kuno, P.V. Kamat, Size-dependent electron injection from excited CdSe quantum dots into TiO_2 nanoparticles, J. Am. Chem. Soc. 129 (2007) 4136–4137.
[10] W.W. Yu, L.H. Qu, W.Z. Guo, X.G. Peng, Experimental determination of the extinction coefficient of CdTe, CdSe, and CdS nanocrystals, Chem. Mater. 15 (2003) 2854–2860.
[11] R. Vogel, P. Hoyer, H. Weller, Quantum-sized PbS, CdS, Ag2S, Sb_2S_3, and Bi_2S_3 particles as sensitizers for various nanoporous wide-bandgap semiconductors, J. Phys. Chem. B 98 (1994) 3183–3188.
[12] H.J. Lee, J.H. Yum, H.C. Leventis, S.M. Zakeeruddin, S.A. Haque, P. Chen, S.I. Seok, M. Grätzel, M.K. Nazeeruddin, CdSe quantum dot-sensitized solar cells exceeding efficiency 1% at full-sun intensity, J. Phys. Chem. C 112 (2008) 11600–11608.
[13] J. Hensel, G.M. Wang, Y. Li, J.Z. Zhang, Synergistic effect of CdSe quantum dot sensitization and nitrogen doping of TiO_2 nanostructures for photoelectrochemical solar hydrogen generation, Nano Lett. 10 (2010) 478–483.
[14] O. Niitsoo, S.K. Sarkar, C. Pejoux, S. Rühle, D. Cahen, G. Hodes, Chemical bath deposited CdS/CdSe-sensitized porous TiO_2 solar cells, J. Photochem. Photobiol. A 181 (2006) 306–313.
[15] Y.L. Lee, Y.S. Lo, Highly efficient quantum-dot-sensitized solar cell based on co-sensitization of CdS/CdSe, Adv. Funct. Mater. 19 (2009) 604–609.
[16] Y.L. Lee, C.F. Chi, S.Y. Liau, CdS/CdSe co-sensitized TiO_2 photoelectrode for efficient hydrogen generation in a photoelectrochemical cell, Chem. Mater. 22 (2010) 922–927.
[17] C.C. Chen, H.W. Chung, C.H. Chen, H.P. Lu, C.M. Lan, S.F. Chen, L.Y. Luo, C.S. Hung, E.W.G. Diau, Fabrication and characterization of anodic titanium oxide nanotube arrays of controlled length for highly efficient dye-sensitized solar cells, J. Phys. Chem. C 112 (2008) 19151–19157.
[18] A. Kongkanand, K. Tvrdy, K. Takechi, M. Kuno, P.V. Kamat, Quantum dot solar cells. Tuning photoresponse through size and shape control of CdSe–TiO_2 architecture, J. Am. Chem. Soc. 130 (2008) 4007–4015.
[19] H.Y. Si, Z.H. Sun, H.L. Zhang, Photoelectrochemical response from CdSe-sensitized anodic oxidation TiO_2 nanotubes, Collids Surf. A 313 (2008) 604–607.
[20] X.F. Gao, W.T. Sun, G. Ai, L.M. Penga, Photoelectric performance of TiO_2 nanotube array photoelectrodes cosensitized with CdS/CdSe quantum dots, Appl. Phys. Lett. 96 (2010) 153104–153106.
[21] M. Paulose, K. Shankar, S. Yoriya, H.E. Prakasam, O.K. Varghese, G.K. Mor, T.A. Latempa, A. Fitzgerald, C.A. Grimes, Anodic growth of highly ordered TiO_2 nanotube arrays to 134 μm in length, J. Phys. Chem. B 110 (2006) 16179–16184.
[22] S.C. Hayden, N.K. Allam, M.A. El-Sayed, TiO_2 nanotube/CdS hybrid electrodes: extraordinary enhancement in the inactivation of *Escherichia coli*, J. Am. Chem. Soc. 132 (2010) 14406–14408.
[23] J.B. Sambur, B.A. Parkinson, CdSe/ZnS core/shell quantum dot sensitization of low index TiO_2 single crystal surfaces, J. Am. Chem. Soc. 132 (2010) 2130–2131.
[24] W.U. Huynh, J.J. Dittmer, A.P. Alivisatos, Hybrid nanorod-polymer solar cells, Science 295 (2002) 2425–2427.
[25] S. Giménez, I. Mora-Seró, L. Macor, N. Guijarro, T.L. Villarreal, R. Gómez, L.J. Diguna, Q. Shen, T. Toyoda, J. Bisquert, Improving the performance of colloidal quantum-dot-sensitized solar cells, Nanotechnology 20 (2009) 295204–295209.
[26] M. Grätzel, Photoelectrochemical cells, Nature 414 (2001) 338–344.
[27] G.V. Chris, J. Neugebauer, Universal alignment of hydrogen levels in semiconductors, insulators and solutions, Nature 423 (2003) 626–628.